

HUMAN ELECTROCORTIGRAPHIC SIGNATURE DETERMINATION BY EGAD SPARSE APPROXIMATION

Jeffrey M. Sieracki ^{a,c}, Nathan E. Crone ^b

John J. Benedetto ^c

^aSR2 Group, LLC
PO Box 1011, College Park, MD 20741

^bDepartment of Neurology
The Johns Hopkins Univeristy School of Medicine
Baltimore, Maryland, 21287

^cNorbert Wiener Center for
Harmonic Analysis and Applications
University of Maryland
Department of Mathematics
College Park, MD 20742

ABSTRACT

Estimated parametric Greedy Adaptive Discrimination (eGAD) is an algorithm for signal-ensemble component analysis based on simultaneous sparse approximation. It is robust against jitter as well as additive noise. We review the algorithm and its application in the context of comparing extracted parametric Gabor atom decompositions to uncorrelated baseline data. We briefly illustrate functionality on synthetic data, before demonstrating application in analysis of multi-channel human electrocortigraphic (ECoG) data. ECoG and muscle (EMG) recordings are analyzed with the goal of identifying characteristic activity patterns associated with simple motor tasks. eGAD compares well with results from previous short time Fourier transform (STFT) based studies, resolving more detail than previous methods where activity increases over baseline and allowing time-domain reconstruction of signature activity where it was not previously possible.

1. INTRODUCTION

Electrocorticography (ECoG) comprises direct recording of electrical signals from the brain surface. In studying the brain, we wish to reliably correlate these electrical signals with behavioral tasks. For purposes of demonstration, we used portions of a dataset previously reported. [1] [2] The data was obtained prior to epilepsy surgery at The Johns Hopkins Hospital. The behavioral task associated with this ECoG is a cued voluntary muscle contraction, in which a subject clenches her fist in response to computer-generated cues. This *active* condition is compared to a passive *baseline*. Previous analysis using windowed short time Fourier transforms (STFT) demonstrated correlated suppression of alpha (8-13 Hz.) and increases in gamma (> 30 Hz.) energy in activated brain areas. We reexamine two channels of ECoG and one channel of EMG over an ensemble of 49 trials. Each trial recording is synchronized to the onset of the visual cue. One cannot expect precise time alignment of the ensemble signals since they are biological in origin and subject to human reaction time variation. The relationship between ECoG and underlying activity cannot easily be predicted due to the enormous complexity of the system. Hence, in empirically determining the electrical signature of behavioral activity, one desires to make as few assumptions as possible as to the nature of the signature, potentially allowing time, phase, amplitude, and frequency to vary due to uncontrolled factors.

For information contact J. Sieracki at SenSIPpaper@sr2group.com.

2. MATHEMATICAL METHODS

Low-dimensional, sparse representations have advantages over decompositions such as the STFT: By concentrating information into fewer, larger coefficients, dimensionality is reduced, round-off error instabilities are minimized, and decision algorithms become more transparent. Sparse representation can also aid in interpretation of signal structure. We are concerned with adaptive approximations of a signal f^i that lie in an appropriate Hilbert space H , termed the *signal space*. Suppose that we adaptively approximate a collection of signals $\{f^i\}_{i=1}^M$ where $M \geq 2$,

$$f^i = a_0^i g_{\gamma_0^i} + a_1^i g_{\gamma_1^i} + \dots + a_n^i g_{\gamma_n^i} + R^i. \quad (1)$$

R^i is the residue (if any) after approximation to $n + 1$ terms, the coefficients a_l^i depend upon the component *atoms* $g_{\gamma_l^i}$, and the collection of atoms $\{g_{\gamma_l^i}\} \subset H$ defines a *representation space* for the decomposition. Typically each $g_{\gamma_l^i}$ belongs to a dictionary, $\mathcal{D} \subset H$, from which sufficient atoms are selected to approximate each f . In general $\{g_{\gamma_l^i}\} \neq \{g_{\gamma_l^j}\}$, so it is not possible to compare directly the representation coefficients of one signal with those of another without further processing. Ideally, we would like to find a representation space such that $g_{\gamma_l^i} = g_{\gamma_l^j}$ for all $l \in (0, n]$ that simultaneously generates sparse approximations for all signals $\{f^i\}_{i=1}^M$.

Sieracki [3] [4] previously developed a series of Greedy Adaptive Discrimination (GAD) algorithms suited to this problem. Certain aspects relate in part to generalizations of Mallat and Zhang's method of Matching Pursuits (MP). [5] [6] GAD introduced an extended Simultaneous Matching Pursuits (SMP) algorithm together with methods for detecting and extracting features from ensembles of signals. Associated theory and methods for analyzing additional classes of data have been elaborated elsewhere. [3] [7] [8] SMP and related sparse approximation topics have generated interest among other authors as well, (c.f.[9],[10].)

For purposes of illustrating the GAD algorithm, SMP may be written as follows:

Definition 1 (Simultaneous Matching Pursuits)

Let $\{f^i\} \subset H$ be indexed by $i \in s$, with $|s| < \infty$.

Let $\mathcal{D} = \{g_\gamma\}_{\gamma \in \Gamma} \subset H$ and $\alpha \in (0, 1]$.

1. Define $R^0 f^i \equiv f^i$.

Set $n = 0$.

2. Find $g_{\gamma_n} \in \mathcal{D}$ such that, for some $i \in s$,

$$\left| \langle R^n f^i, g_{\gamma_n} \rangle \right| \geq \alpha \sup_{\gamma \in \Gamma} \left| \langle R^n f^i, g_\gamma \rangle \right|. \quad (2)$$

3. Project $R^n f^i$ on g_{γ_n} to find $R^{n+1} f^i$ for all $i \in s$ by

$$R^n f^i = \langle R^n f^i, g_{\gamma_n} \rangle g_{\gamma_n} + R^{n+1} f^i. \quad (3)$$

4. Repeat steps 2 and 3 for $(n+1)^{th}$ residue, etc.

SMP in the case of $\text{card}(\{f^i\}) = |s| = 1$, with Mallat and Zhang's choice function, is precisely MP.[5] The more general GAD choice function is based on a vector p-norm over the ensemble:

Definition 2 (p-norm) Given $n \in \mathbb{N}$ and $\gamma \in \Gamma$. For each vector $\{\langle R^n f^i, g_\gamma \rangle\}_{i \in s} = (\langle R^n f^1, g_\gamma \rangle, \langle R^n f^2, g_\gamma \rangle, \dots, \langle R^n f^{|s|}, g_\gamma \rangle) \in \mathbb{C}^{|s|}$, let the p-norm for positive integer p be defined by

$$\left\| \left\{ \langle R^n f^i, g_\gamma \rangle \right\} \right\|_p = \left(\sum_{i \in s} \left| \langle R^n f^i, g_\gamma \rangle \right|^p \right)^{\frac{1}{p}}. \quad (4)$$

Definition 3 (GAD Choice Function)

1. Find $g_{\bar{\gamma}_n} \in \mathcal{D}_\alpha$ such that,

$$\left\| \left\{ \langle R^n f^i, g_{\bar{\gamma}_n} \rangle \right\} \right\|_p = \sup_{\gamma \in \Gamma_\alpha} \left\| \left\{ \langle R^n f^i, g_\gamma \rangle \right\} \right\|_p; \quad (5)$$

2. For each $i \in s$, search in a neighborhood $N_{g_{\bar{\gamma}_n}}$ of $g_{\bar{\gamma}_n}$ for $g_{\gamma_n^i} \in \mathcal{D}$ for which $\left| \langle R^n f^i, g_{\gamma_n^i} \rangle \right|$ reaches a local maximum.

Correspondingly, we replace the update step relationship (3) with

$$R^n f^i = \langle R^n f^i, g_{\gamma_n^i} \rangle g_{\gamma_n^i} + R^{n+1} f^i. \quad (6)$$

Fit is optimized for each residue in the ensemble. With this choice function replacing (2), convergence is exponential for any p . [3]. Other norms may also be considered. We utilize a 2-norm in this study, which empirically outperforms the 1-norm and ∞ -norm in the signature extraction application.[7]

We store the resulting representation in a generalized structure book, indexing the atoms as well as the coefficients with $i \in s$:

$$\left\{ \left\{ \langle R^n f^i, g_{\gamma_n^i} \rangle \right\}_{i \in s}, \left\{ \gamma_n^i \right\}_{i \in s} \right\} n \in \mathbb{N}. \quad (7)$$

Each subset $\left\{ g_{\gamma_n^i} \right\}_{i \in s}$ comprises an equivalence class of similar atoms. Introducing equivalence classes into the simultaneous representation space allows the algorithm to compensate for noise, time jitter, and other variations. We utilize this property in analyzing ECoG data to effectively de-blur the noisy signal ensemble and deduce underlying properties of the source signal. We recover estimates of the source components by reducing each equivalence class to a best estimate of the generating atom. This is accomplished using a Gabor dictionary parameterized by $\gamma = (s, u, \xi)$, corresponding to scale, position, modulation.

Definition 4 (Gabor Dictionary) Let $g(t) = 2^{\frac{1}{4}} e^{-\pi t^2}$ be the Gaussian window function. Let $\gamma = (s, u, \xi)$. The elements of the Gabor Dictionary are those functions $\mathcal{D} = \{g_\gamma(t)\}_{\gamma \in \Gamma} \subset L^2(\mathbb{R})$, defined by

$$g_\gamma(t) = \frac{1}{\sqrt{s}} g\left(\frac{t-u}{s}\right) e^{i\xi t}. \quad (8)$$

This dictionary has useful properties for unbiased signal analysis since the generating Gaussian window is well localized in the time-frequency plane. However, an important characteristic for our purposes is that the generated atoms behave smoothly under parametric variation. Hence, it becomes meaningful to take averages in these parameters over groups of signals.

Definition 5 (Parametric Mean) Let $M = |s|$ be the cardinality of a group of signals. For each n , create a mean structure book entry $(\bar{a}_n, \bar{\gamma}_n)$ where $\bar{\gamma}_n = (\bar{s}_n, \bar{u}_n, \bar{\xi}_n, \bar{\phi}_n)$ and

$$\begin{aligned} \bar{a}_n &= \frac{1}{M} \sum_i \langle R^n f^i, g_{\gamma_n^i} \rangle \\ \bar{s}_n &= \frac{1}{M} \sum_i s_n^i \\ \bar{u}_n &= \frac{1}{M} \sum_i u_n^i \\ \bar{\xi}_n &= \frac{1}{M} \sum_i \xi_n^i \\ \bar{\phi}_n &= \frac{1}{M} \sum_i \phi_n^i. \end{aligned} \quad (9)$$

Other meaningful operations may be defined and are discussed in [3] and [8]. We have shown phase ϕ explicitly since our examples are real-valued signals. We term the method of estimating parameters of a source signal through analyzing the parameter space of atoms in GAD equivalence classes *estimated parametric GAD*, or eGAD.

We shall apply the parametric mean to estimate common underlying source elements in active-condition ECoG signals. Our goal is to compare active signals to a passive baseline period during which we assume ECoG signals are uncorrelated. After running GAD, each of the mean-parametric active condition atoms can be matched to the baseline set, asking, in effect, how often and at what energy do similar atoms occur *anywhere* in the baseline data. For the collection of discrete baseline signals $f^i \in \ell^2([0, N-1])$ consider the expression,

$$b_n^2 = \frac{1}{M} \sum_{i \in s^-} \frac{1}{N} \sum_{u=0}^{N-1} \left| \langle f^i, g_{(\bar{s}_n, u, \bar{\xi}_n)} \rangle \right|^2. \quad (10)$$

b_n is then the RMS baseline amplitude for the scale and frequency associated with the n^{th} mean atom, and b_n^2 is an estimate of the expected value of energy. (We note this estimate exhibits scale dependant bias, which is not of concern in this application. See [3].)

Using this estimate, one can re-scale each active-condition parametric mean atom to show deviation in energy from uncorrelated baseline activity.

$$\underline{a}_n = \frac{\bar{a}_n^2 - b_n^2}{b_n^2}. \quad (11)$$

To extract significant signal elements one may threshold the resulting structure book, retaining only those atoms $g_{\bar{\gamma}_{n_\ell}}$ for which the corresponding proportionately re-scaled amplitude $\underline{a}_{n_\ell} > \epsilon$. Finally, one may reconstruct a representative time-domain signal from the resulting subsequence of extracted elements $\{\bar{a}_{n_\ell}, g_{\bar{\gamma}_{n_\ell}}\}_{n \in \{n_\ell\}}$ using

$$\bar{f}(t) = \sum_{n_\ell} \bar{a}_{n_\ell} g_{\bar{\gamma}_{n_\ell}}(t), \quad (12)$$

where $\{n_\ell\}$ indexes the parametric-mean atoms of interest from the analysis.

In the next sections we demonstrate these operations on both synthetic and actual ECoG recordings.

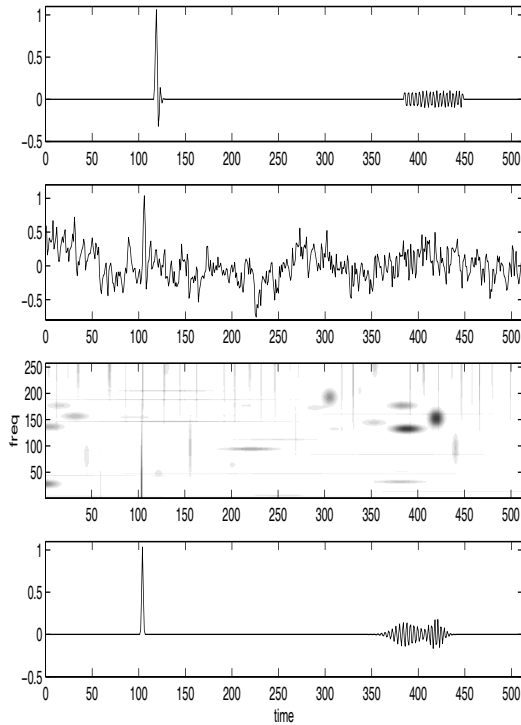


Fig. 1. Signal recovery example, showing (top to bottom) the model signal, 1 of 5 noisy samples in the ensemble, T-F energy increases over baseline, and a recovered estimate of the model signal.

3. SYNTHETIC DATA

Figure 1 illustrates the operation on a synthetic example. The model signal (shown at top) comprised a short transient and a brief linear chirp segment in a 512 point window. These components cannot be exactly reconstructed with a small number of Gabor atoms.

The signal was translated by random walk ($\mu = 0, \sigma = 10$) five successive times, producing five time-jittered signals that drifted a total of about 20 time points to the left of the original. Each of the five samples was further degraded with additive $1/f$ noise. The second plot shows one example of a noisy signal in the ensemble of five. To form a baseline comparison set, five additional $1/f$ noise samples were generated without the model signal present.

An eGAD type SMP analysis was performed on the noisy signal ensemble, with parameters set to allow up to ± 10 points of jitter within an equivalence class. The third plot shows the re-scaled Wigner energy density (see [11] and [5]) of only those extracted mean-parametric components that increased over baseline (i.e., $\underline{a}_{n\ell} > 0$). Both the transient and the upward chirp are identified by strong components in the expected T-F regions.

After thresholding to retain only the largest re-scaled elements, the recovered mean parametric atoms are summed using equation (12) to obtain a time-domain estimate of the underlying source signal. The bottom plot of Figure 1 shows the recovered approximation. The reconstruction is translated to the left relative to the model signal, reflecting the random-walk drift of the ensemble of samples. Nonetheless, the basic signal elements and the spacing between elements are recovered to a good approximation.

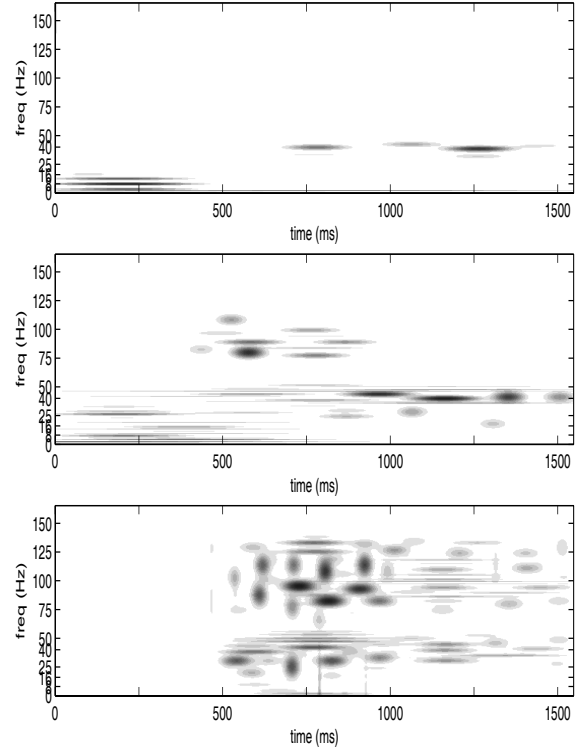


Fig. 2. Wigner T-F energy density for significant parametric-mean atoms for channels 19 (top), 20 (middle), and the EMG (bottom). [Reprinted with permission of J. Sieracki]

4. ECG RESULTS

ECoG data was collected from electrodes over brain regions associated with the fist-clenching task. The behavioral task is summarized in the introduction above. The data was originally analyzed using a windowed STFT; for full details of the original study, see [1] and [2]. The data has been reanalyzed by other methods as well (c.f., [12]). For the present example we selected two channels of data that showed reliable correlated activity.

The task comprised 49 fist-clenching trials. ECoG recordings for each trial were segmented and aligned based on the onset time of the visual cue. Note that for the present analysis, data was not pre-filtered to narrow the frequency band or to remove known noise sources as it was in [1] and [2]. Otherwise, the example data correspond to channels 19 and 20 in that larger study.

For this eGAD analysis, the active set for each channel comprised ECoG from the cue onset to a period 1.55 seconds post cue onset. Baseline data for each channel comprised the collection of ECoG segments just before cue onset. Only 1.0 second of pre-cue data was available, so data was treated as periodic in order to normalize window length.

In addition to ECoG, an EMG channel showing muscle activity associated with fist-clenching was also available. The EMG signals are added as a third ensemble in the analysis to provide a direct comparison between the measured brain activity and the physical action.

An eGAD type SMP analysis was performed on each of the three ensembles of 49 active signals. Parameters were set to allow a variance of ± 45 ms time jitter within an equivalence class, allowing a

maximum of 90 ms of time offset between any two related signals.

It is well known that the original MP formulation [5] [6] is not a fast algorithm in comparison to fixed decompositions like the FFT. However, redundancy of information across the ensembles significantly speeds convergence for our SMP methods. All significant atoms in the present ECoG analysis were recovered in less than 200 iterations. This produces a highly sparse, low dimensional representations of each signal ensemble.

Recovered signal components were re-scaled according to the estimated baseline energy, as discussed in the Section 2, and those corresponding to increases over baseline are presented here.

Figure 2 shows Wigner energy distribution for the re-scaled parametric-mean atoms plotted for channels 19 and 20 of ECoG and for the EMG channel. The results are consistent with the originally measured time course in [1] and [2]. In the ECoG channels, lower frequency (alpha band) energy is prevalent during resting stages and prior to the onset of muscle motion, while higher frequency (gamma band) energy is prevalent during muscle motion. However, for those portions of the time-frequency plane that are active, eGAD reveals striking detail when compared to the resolution of the STFT study in [1] and [2]. Time-frequency correlations between the EMG and the cortical activity are easily examined in the plots. In addition we were able to isolate and easily eliminate artifact signals from the raw recordings (not shown.)

Weakly represented time-frequency plane regions are inherently downplayed by the greedy algorithm; hence, the method as presented here will not fully characterize energy suppression relative to baseline. This is relevant since alpha-band suppression is considered important in the literature (c.f., [1]). We note, however, that since the alpha energy is dominant prior to activity onset in the illustrated examples, suppression is in fact clear from the plots in figure 2 and numerical comparisons can be made by other means outside the scope of this paper.

Using the same atoms illustrated in figure 2, time-domain parametric-mean signature signals are reconstructed and plotted in figure 3 for the two channels of ECoG. The time-domain average of the EMG signal is shown at the bottom for comparison. These plots may represent a reasonable first approximation to the ECoG signature activity associated with fist-clenching in this patient.

A notable feature of eGAD analysis in contrast to other techniques for analyzing event-related spectral changes, is that we retain enough information to reconstruct a representative time-domain signal. As demonstrated in the synthetic example, this reconstruction is a reasonable approximation of the common underlying source signal. Hence, one may potentially extract both spectrographic and time-domain signatures with the reported method.

5. REFERENCES

- [1] N. Crone, D. Miglioretti, B. Gordon, J. Sieracki, M. Wilson, S. Uematzu, and R. Lesser, "Functional mapping of human sensorimotor cortex with electrocorticographic spectral analysis," *Brain*, vol. 121, pp. 2271–2299, 1998.
- [2] N. Crone, D. Miglioretti, B. Gordon, and R. Lesser, "Functional mapping of human sensorimotor cortex with electrocorticographic spectral analysis II. Event-related synchronization in the gamma band," *Brain*, vol. 121, pp. 2301–2315, 1998.
- [3] J. M. Sieracki, *Greedy Adaptive Discrimination: Signal component analysis by simultaneous matching pursuits with application to ECoG signature detection.*, PhD dissertation, University of Maryland, College Park, 2002.

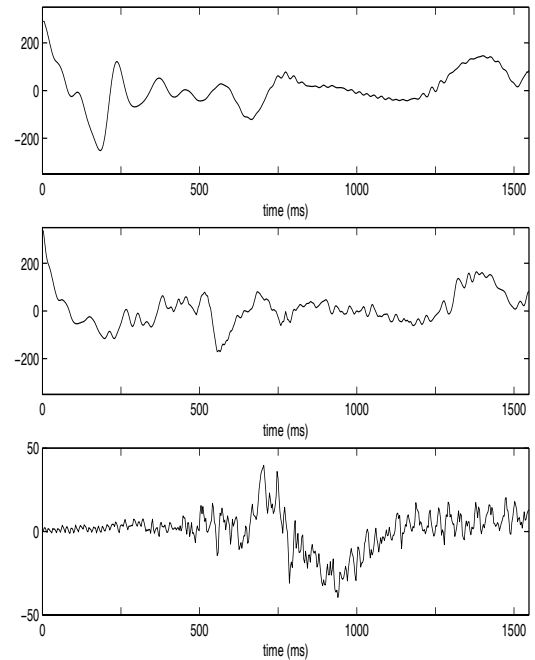


Fig. 3. Reconstructed parametric-mean signatures for channels 19, 20, and the time domain average of EMG. [Reprinted with permission of J. Sieracki]

- [4] J. M. Sieracki, *Greedy Adaptive Signature Discrimination System and Method*, United States Patent, US 7,079,986 B2.
- [5] S. Mallat and Z. Zhang, "Matching pursuits with time-frequency dictionaries," *IEEE Transactions on Signal Processing*, vol. 41, no. 12, pp. 3397–3415, Dec. 1993.
- [6] G. M. Davis, S. Mallat, and M. Avelanedo, "Greedy adaptive approximations," *J. of Constr. Approx.*, vol. 13, pp. 57–98, 1997.
- [7] J. M. Sieracki and J. J. Benedetto, "Greedy adaptive discrimination: component analysis by simultaneous sparse approximation," *Proc. of SPIE*, vol. 5914, pp. 59141R, 2005.
- [8] J. M. Sieracki and J. J. Benedetto, "Greedy adaptive discrimination by simultaneous matching pursuits," *In preparation*.
- [9] J. A. Tropp, A. C. Gilbert, and M. J. Strauss, "Simultaneous sparse approximation via greedy pursuit," *Proc. ICASP, Philadelphia*, 2005.
- [10] D. Leviatan and V.N. Temlyakov, "Simultaneous approximations by greedy algorithms," 2003, vol. 2003:02, Univ. of South Carolina at Columbia.
- [11] L. Cohen, "Time-frequency distributions – A review," *Proc. IEEE*, vol. 77, pp. 941–981, 1989.
- [12] J. Zygierevicz, P.J. Durka, H. Klekowicz, P.J. Franaszczuk, and N.E. Crone, "Computationally efficient approaches to calculating significant ERD/ERS changes in the time frequency plane," *J. Neurosci Methods*, vol. 145, pp. 267–276, 2005.

Methods and algorithms are subject to US and international patent protection. Contact SR2 Group, LLC for information.